

Reactions of (Butadiene)tantalocene Cation with Alkyl Isocyanides

Hans Christian Strauch, Birgit Wibbeling,[†] Roland Fröhlich,[†] and Gerhard Erker*

Organisch-Chemisches Institut der Universität Münster,
Corrensstrasse 40, D-48149 Münster, Germany

Heiko Jacobsen[‡] and Heinz Berke*[‡]

Anorganisch-Chemisches Institut der Universität Zürich, Winterthurer Strasse 190,
CH-89057 Zürich, Switzerland

Received March 29, 1999

Treatment of (η^4 -*s-trans*-butadiene)tantalocene cation (**3**, with methyltris(pentafluorophenyl)borane anion) with *tert*-butyl isocyanide (4 h, at 45 °C in bromobenzene) yields the [η^2 -butadiene)(C≡NCMe₃)TaCp₂⁺] complex **4a** (70% isolated, $\tilde{\nu}(\text{C}\equiv\text{NR})$ 2164 cm⁻¹). Likewise treatment with *n*-butyl or cyclohexyl isocyanide gives the analogous products **4b** and **4c**, respectively. The cyclohexyl isocyanide adduct **4c** was characterized by X-ray diffraction. It shows the η^2 -butadiene ligand oriented at the front of the Cp₂Ta⁺ bent metallocene wedge with the noncoordinated butadiene vinyl group located in the “vinyl-inside” position. The Ta–C≡N–R unit is almost linear (angles Ta–C–N = 177.2(5)°, C≡N–R = 174.0(8)°; $d(\text{C}\equiv\text{N})$ = 1.152(6) Å). Photolysis of [(butadiene)TaCp₂⁺] (**3**) with excess cyclohexyl isocyanide followed by thermal treatment gave rise to the formation of [bis(κ -C-cyclohexyl isocyanide)-TaCp₂⁺] (**8**, with [CH₃B(C₆F₅)₃⁻] counteranion; > 50% isolated, $\tilde{\nu}(\text{C}\equiv\text{NR})$ 2134 and 2088 cm⁻¹). Complex **8** was characterized by an X-ray crystal structure analysis. It shows a pseudo-tetrahedral [Cp₂Ta(C≡NR)₂⁺] cation (R = C₆H₁₁). The Ta–C≡N–R units are both slightly bent at nitrogen (angles C≡N–R = 169.0(13) and 163.7(8)°; the corresponding Ta–C–N angles are 179.4(9) and 177.4(7)°). The bonding situations of complexes **4** and **8** were analyzed by DFT calculations. The computational study shows that metal to isonitrile back-bonding does not contribute significantly to the Cp₂Ta⁺–C≡NR bonding interaction in these complexes. The bonding between Cp₂Ta⁺ and the C≡NR ligands is dominated by electrostatic effects.

Introduction

(η^4 -Conjugated diene)zirconocene and -hafnocene complexes have found interesting applications in organic synthesis and in catalysis.¹ Several studies have been reported where these reagents were treated with the C₁-building blocks carbon monoxide or alkyl or aryl isocyanides (RN≡C). In most of these cases incorporation of CO/C≡NR is observed, leading to carbon–carbon coupling with the conjugated diene ligand, and ultimately cyclopentenone formation is often achieved.² Only in a few exceptional examples can 1,3-diene

extrusion with formation of the respective Cp₂M^{II} complexes (e.g. Cp₂Zr(CO)₂) compete.³

We have recently prepared the group 5 analogue of these (1,3-diene) bent-metallocene systems, namely (butadiene)tantalocene cation (**3**). We have shown that only the [η^4 -*s-trans*-C₄H₆)TaCp₂]⁺ isomer is stable and is observed at ambient temperature. It inserts a variety of unsaturated reagents (ketones, nitriles, alkynes) to form the respective metallacyclic (π -allyl)- or the seven-membered (σ -allyl)metallocene complexes, similar to the way their neutral group 4 metallocene analogues react with these reagents.⁴ We have now treated (butadiene)-

* To whom correspondence should be addressed. G.E.: FAX, +49 251 83 36 503; E-mail, erker@uni-muenster.de. H.B.: FAX, +41 1 635 4680; E-mail, hberke@aci.unizh.ch.

[†] X-ray crystal structure analyses.

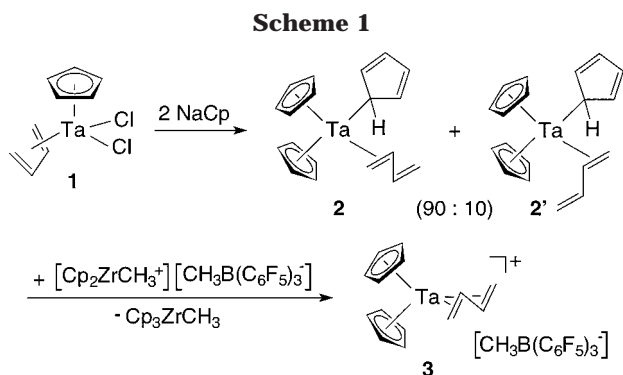
[‡] Quantum-chemical calculations.

(1) (a) Erker, G.; Pfaff, R.; Krüger, C.; Nolte, M.; Goddard, R. *Chem. Ber.* **1992**, *125*, 1669. Erker, G.; Pfaff, R. *Organometallics* **1993**, *12*, 1921. Erker, G.; Pfaff, R.; Kowalski, D.; Würthwein, E.-U.; Krüger, C.; Goddard, R. *J. Org. Chem.* **1993**, *58*, 6771. Berlekamp, M.; Erker, G.; Schönecker, B.; Krieg, R.; Rheingold, A. L. *Chem. Ber.* **1993**, *126*, 2119. Erker, G.; Berlekamp, M.; López, L.; Grehl, M.; Schönecker, B.; Krieg, R. *Synthesis* **1994**, 212. (b) Temme, B.; Erker, G.; Karl, J.; Luftmann, H.; Fröhlich, R.; Kotila, S. *Angew. Chem.* **1995**, *107*, 1867; *Angew. Chem., Int. Ed. Engl.* **1995**, *34*, 1755. Karl, J.; Dahlmann, M.; Erker, G.; Bergander, K. *J. Am. Chem. Soc.* **1998**, *120*, 5643.

(2) (a) Erker, G.; Engel, K.; Krüger, C.; Chiang, A.-P. *Chem. Ber.* **1982**, *115*, 3311. Hessen, B.; Teuben, J. H. *J. Organomet. Chem.* **1988**, *358*, 135. Hessen, B.; Blenkins, J.; Teuben, J. H.; Helgesson, G.; Jagner, S. *Organometallics* **1989**, *8*, 830, 2809. Yasuda, H.; Okamoto, T.; Matsuoka, Y.; Nakamura, A.; Kai, Y.; Kanehisa, N.; Kasai, N. *Organometallics* **1989**, *8*, 1139. (b) For related reactions see e.g.: Hicks, F. A.; Kablaoui, N. M.; Buchwald, S. L. *J. Am. Chem. Soc.* **1996**, *118*, 9450. Hicks, F. A.; Buchwald, S. L. *J. Am. Chem. Soc.* **1996**, *118*, 11688. Takahashi, T.; Xi, Z.; Nishihara, Y.; Huo, S.; Kasai, K.; Aoyagi, K.; Denisov, V.; Negishi, E. *Tetrahedron* **1997**, *53*, 9123.

(3) Erker, G.; Krüger, C.; Müller, G. *Adv. Organomet. Chem.* **1985**, *24*, 1. Beckhaus, R.; Wilbrandt, D.; Flatan, S.; Böhmer, W.-H. *J. Organomet. Chem.* **1992**, *423*, 211.

(4) Strauch, H. C.; Erker, G.; Fröhlich, R. *Organometallics* **1998**, *17*, 5746.



tantalocene cation (**3**) with a small series of isocyanide reagents RN≡C under various reaction conditions and observed a quite different behavior and outcome of these reactions. These observations are described in this article.

Results and Discussion

Thermally Induced Reactions of (Butadiene)-tantalocene with Alkyl Isocyanides. (η^4 -*s-trans*-Butadiene)tantalocene cation (**3**) was prepared according to the synthetic route that we have recently developed,⁴ starting from (η^4 -*s-cis*-butadiene)(η^5 -cyclopentadienyl)tantalum dichloride (**1**).⁵ Treatment with 2 molar equiv of sodium cyclopentadienide gave [$(\eta^5$ -Cp)₂(η^1 -Cp)(η^2 -butadiene)Ta] (**2**), which was subsequently treated with [Cp₂ZrCH₃⁺][CH₃B(C₆F₅)₃⁻].⁶ A clean Cp transfer was achieved to yield the desired [(C₄H₆)/TaCp₂]⁺ cation (**3**, with [CH₃B(C₆F₅)₃]⁻ anion), which was easily separated from the stoichiometrically formed neutral coproduct Cp₃ZrCH₃⁷ (see Scheme 1).

[(butadiene)TaCp₂]⁺ cation (**3**) was then treated with a variety of alkyl isocyanides to cleanly yield the respective 1:1 addition products. The reaction between **3** and *tert*-butyl isocyanide takes place readily in bromobenzene solution at elevated temperature. The reaction is complete after 4 h at 45 °C, and the product (**4a**) was isolated in close to 70% yield as a red solid. The IR spectrum shows the $\tilde{\nu}$ [C≡N(R)] band at 2164 cm⁻¹, which is ca. 25 cm⁻¹ shifted to *higher* wavenumbers from the value of the free *tert*-butyl isocyanide.^{8,16} The ¹H and ¹³C NMR data show that the butadiene ligand was shifted into a η^2 -coordination⁹ by the attachment of the additional donor ligand at the central tantalum atom. This has resulted in the formation of a center of chirality (at the carbon atom C2 of the η^2 -butadiene

ligand). Consequently, the ¹H/¹³C NMR resonances of a pair of diastereotopic η^5 -cyclopentadienyl ligands at the cationic Ta complex **4a** are observed (δ 4.69, 4.68/96.8, 96.5 ppm in bromobenzene-*d*₅ at 298 K and 600/150 MHz).

The reactions between [(butadiene)TaCp₂]⁺ (**3**) and *n*-butyl isocyanide or cyclohexyl isocyanide proceed equally well to give high yields of the respective 1:1 addition products **4b** and **4c**. In each case a single 1:1 reaction product is obtained. In principle, the addition of the isocyanide ligand to the bent-metalocene cation complex **3** could have resulted in the formation of two diastereoisomeric [(η^2 -butadiene)Ta(L)Cp₂]⁺ cation complexes (L = RN≡C). These would differ in their relative positions of the uncoordinated butadiene vinyl moiety; the complexes **4** exhibit the vinyl-substituted η^2 -butadiene carbon C2 in the central position in the σ -ligand plane at the bent metalocene wedge, whereas the isomer **4'** would show this in a lateral position (Scheme 2).¹⁰ In each case, we have observed the formation of only a single isomer. The product formed by the addition of cyclohexyl isocyanide to **3** again shows the ¹H/¹³C NMR signals of a pair of diastereotopic Cp ligands at tantalum. Its ¹³C NMR spectrum is characterized by the presence of four butadiene carbon resonances, two at large δ values in the typical olefinic region (δ 141.3, 111.1). These belong to the noncoordinated butadiene vinyl group (C3, C4). The remaining pair of butadiene ligand carbon signals are observed at much smaller δ values (δ 23.1, 43.6 ppm; C1, C2) as is typical for a metal-coordinated butadiene -CH=CH₂ unit.¹¹ A similar distinction between the butadiene ligand sections is observed in the ¹H NMR spectra of the [(η^2 -butadiene)-(C₆H₁₁N≡C)TaCp₂]⁺ product. Three signals of the coordinated -C²H=C¹H₂ moiety are observed at high field (δ 1.62, 1.58, 2.60 (1-H'/H; 2-H) with coupling constants of ²J = 5.5 Hz, ³J = 12.9 and 10.1 Hz). The noncoordinated -C³H=C⁴H₂ moiety exhibits corresponding ¹H NMR resonances at δ 5.39, 4.90, and 4.67 ppm (3-H, 4-H'/H) with coupling constants of ³J = 16.7 and 9.9 Hz. The NMR spectra show that in each case a single product was formed, but they do not allow for a clear structural assignment as to which of the two, the "vinyl-inside" (**4**) or "vinyl-outside" isomer (**4'**),¹⁰ was actually obtained. Fortunately, we have obtained single crystals of two of the complexes, namely the *n*-butyl-N≡C and the cyclohexyl-N≡C adducts, which allowed for a characterization by X-ray crystal structure analyses. Both clearly showed the presence of the "vinyl-inside"

(5) Yasuda, H.; Tatsumi, K.; Okamoto, T.; Mashima, K.; Lee, K.; Nakamura, A.; Kai, Y.; Kanehisa, N.; Kasai, N. *J. Am. Chem. Soc.* **1985**, *107*, 2410.

(6) Yang, X.; Stern, C. L.; Marks, T. J. *J. Am. Chem. Soc.* **1994**, *116*, 10015.

(7) Brackemeyer, T.; Erker, G.; Fröhlich, R. *Organometallics* **1997**, *16*, 531.

(8) For related effects in d⁰-configured metal isocyanide complexes see e.g.: Guo, Z.; Swenson, D. C.; Guram, A. S.; Jordan, R. F. *Organometallics* **1994**, *13*, 766 and references therein. See also: Hurlburt, P. K.; Rack, J. J.; Luck, J. S.; Dec, S. F.; Webb, J. D.; Anderson, O. P.; Strauss, S. H. *J. Am. Chem. Soc.* **1994**, *116*, 10003. Antonelli, D. M.; Tjaden, E. B.; Stryker, J. M. *Organometallics* **1994**, *13*, 763. Guram, A. S.; Swenson, D. C.; Jordan, R. F. *J. Am. Chem. Soc.* **1992**, *114*, 8991.

(9) Thomas, J. L. *Inorg. Chem.* **1978**, *17*, 1507. Sen, A.; Halpern, J. *Inorg. Chem.* **1980**, *19*, 1073. Beck, W.; Raab, K.; Nagel, U.; Sacher, W. *Angew. Chem.* **1985**, *97*, 498; *Angew. Chem., Int. Ed. Engl.* **1985**, *24*, 505. Peng, T.-S.; Wang, Y.; Arif, A. M.; Gladysz, J. A. *Organometallics* **1993**, *12*, 4535.

(10) For related situations see e.g.: Erker, G. *Acc. Chem. Res.* **1984**, *17*, 103, and references therein. Tatsumi, K.; Nakamura, A.; Hofmann, P.; Stauffert, P.; Hoffmann, R. *J. Am. Chem. Soc.* **1985**, *107*, 4440.

(11) Burger, B. J.; Santarsiero, B. D.; Trimmer, M. S.; Bercaw, J. E. *J. Am. Chem. Soc.* **1988**, *110*, 3134.

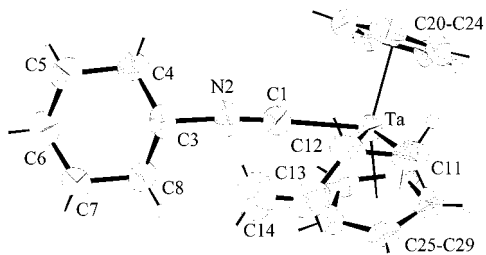


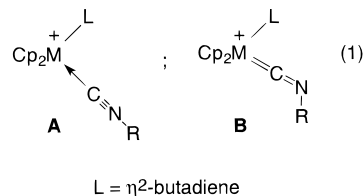
Figure 1. Molecular structure of **4c** (cation only) with nonsystematic atom-numbering scheme. Selected bond lengths (Å) and angles (deg): Ta–C1 = 2.118(6), Ta–C11 = 2.314(5), Ta–C12 = 2.392(6), Ta–C13 = 3.288(8), C1–N2 = 1.152(6), N2–C3 = 1.461(7), C11–C12 = 1.416(9), C12–C13 = 1.435(10), C13–C14 = 1.349(10); Ta–C1–N2 = 177.2(5), C1–N2–C3 = 174.0(8), C11–Ta–C12 = 35.0(2), Ta–C11–C12 = 75.5(3), Ta–C12–C11 = 69.5(3), Ta–C12–C13 = 116.2(5), C11–C12–C13 = 122.8(8), C12–C13–C14 = 124.2(8).

isomers **4b,c**. The structure of the *n*-BuNC adduct suffered from some disorder problems, and so will not be discussed here, but the **4c** structure was of a sufficient quality for a characterization of this class of compounds.

The X-ray crystal structure analysis of complex **4c** shows well-separated anion (i.e. $\text{CH}_3\text{B}(\text{C}_6\text{F}_5)_3^-$) and cation moieties (Figure 1). The cation of **4c** exhibits a bent-metallocene unit (Cp(centroid)–Ta–Cp(centroid) angle 134.9°) to which a κ -isonitrile and a η^2 -butadiene ligand are coordinated, both at the front side of the bent-metallocene wedge.¹² The η^2 -butadiene ligand is bonded such that the free vinyl group is oriented in the central position (“vinyl-inside” position). The free vinyl group shows the expected bond lengths and angles: 1.349(10) Å (C13–C14), 1.435(10) Å (C12–C13), $124.2(8)^\circ$ (C12–C13–C14), which are similar to free 1,3-butadiene (C1–C2 = 1.334 Å; C2–C3 = 1.416 Å).¹³ The coordinated butadiene double bond is substantially elongated (C11–C12 = 1.416(9) Å). The C11–C12–C13 angle is $122.8(8)^\circ$, and the C11–C12–C13–C14 torsional angle is $163.6(7)^\circ$. This ca. 16° deviation from the butadiene θ value already indicates some metallacyclopropane character of the Ta(η^2 -C₄H₆) linkage, as is commonly observed for many early-transition-metal η^2 -alkene complexes.¹⁴ Consequently, the Ta–C11 (2.314(5) Å) and Ta–C12 (2.392(6) Å) bonds are approaching a metal–carbon σ -bond range.

The cyclohexyl isocyanide ligand is bonded to tantalum at a lateral position in the major coordination plane at the front sector of the bent-metallocene wedge (C1–Ta–C11 = $107.3(3)^\circ$). The –N≡C substituent is oriented at the cyclohexyl chair in an equatorial position. The C3–N2 bond length is 1.461(7) Å, and the Ta–C1 bond is 2.118(6) Å. The C1–N2 linkage is in the typical range of a carbon–nitrogen triple bond at 1.152(6) Å. The Ta–C1–N2 moiety is very close to linear ($177.2(5)^\circ$). More importantly, the C1–N2–C3 angle ($174.0(8)^\circ$) also does not deviate much from linear. Together with the typical

IR (C≡N(cyclohexyl)) stretching band at $\tilde{\nu}$ 2174 cm^{-1} , which is slightly *increased* relative to the free, uncoordinated isonitrile, these data indicate that the Cp_2Ta^+ –isonitrile coordination is lacking any substantial back-bonding component.¹⁵ The bonding situation of the metallocene–isonitrile linkage is probably more adequately represented by the description **A** in eq 1 than



by **B**. The latter represents a situation where metal to carbon back-bonding is substantial,¹⁶ whereas **A** characterizes a metal/ligand arrangement that is probably dominated by electrostatic bonding effects.¹⁵

Metal to isonitrile back-bonding would be indicated by both a *decrease* of the $\tilde{\nu}(\text{C}\equiv\text{N}-)$ IR band of the coordinated C≡NR ligand relative to the free isonitrile and a substantial bending of the coordinated C≡NR unit at the central nitrogen atom.¹⁶ Both features are clearly absent in the complexes **4**. We conclude that tantalum to isonitrile carbon back-bonding is negligible in the cation complexes **4** and that the Cp_2Ta^+ –C≡NR bonding situation is likely to be characterized by a large electrostatic contribution. Formally the metal in the systems **4** has a d^2 configuration Ta(III), but the pronounced metallacyclopropane character of the (η^2 -butadiene)Ta subunit may have shifted the system toward a pronounced d^0 Ta(V) character.¹⁴ We have, therefore, tried to substitute the η^2 -butadiene for a second isonitrile ligand and characterize the bonding features of the resulting formally d^2 -configured $[\text{Cp}_2\text{Ta}(\text{L})_2]^+$ systems. It turned out that we had to use a photochemical synthetic route to prepare such a system starting from the (*s-trans*- η^4 -butadiene)tantalocene cation (**3**).

Photochemically Induced Reactions of (*s-trans*- η^4 -Butadiene)tantalocene Cation. Scouting experiments have revealed that the butadiene ligand can rather easily be removed from **3** by photolysis in the presence of suitable donor ligands. Thus, when a sample of $[(\eta^4\text{-butadiene})\text{TaCp}_2]^+$ (**3**) was irradiated (Philips HPK 125 lamp, Pyrex filter) in THF-*d*₈ (ca. 80 mg of **4** in 0.8 mL of solvent) at -78°C for ca. 1 h, a 55:10:5:30 mixture of the products **3** (i.e. residual starting material), **5**, **5'**, and **6** (plus free butadiene) was obtained. The products **5** and **5'** both contained a η^2 -butadiene ligand coordinated to tantalum, as is evident from their very characteristic NMR data (see Table 1), and each of them exhibits a pair of diastereotopic Cp ligands. The nature of the additional donor ligand is not completely clear. We have observed the low-intensity signals of

(12) Lauher, W.; Hoffmann, R. *J. Am. Chem. Soc.* **1976**, *98*, 1729.
(13) Allen, F. H.; Kennard, O.; Watson, D. G.; Brammer, L.; Orpen, A. G.; Taylor, R. *J. Chem. Soc., Perkin Trans. 2* **1987**, S1.

(14) Dewar, M. J. S.; Dougherty, R. C. *The PMO Theory of Organic Chemistry*; Plenum Press: New York, 1975; p 300. Dewar, M. J. S.; Ford, G. P. *J. Am. Chem. Soc.* **1979**, *101*, 783 and references therein. Cremer, D.; Kraka, E. *J. Am. Chem. Soc.* **1985**, *107*, 3800.

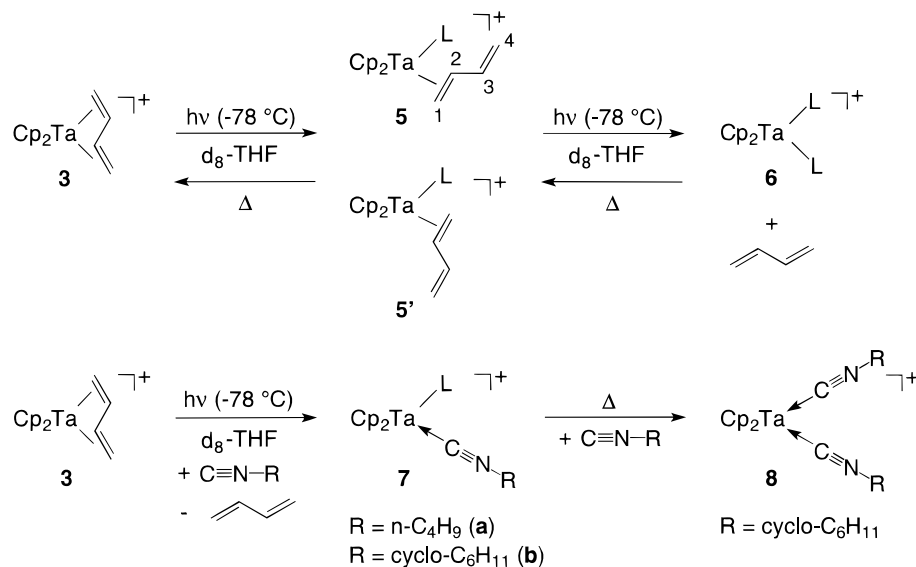
(15) (a) Jacobsen, H.; Berke, H.; Döring, S.; Kehr, G.; Erker, G.; Fröhlich, R.; Meyer, O. *Organometallics* **1999**, *18*, 1724. (b) Jacobsen, H.; Berke, H.; Brackemeyer, T.; Eisenblätter, T.; Erker, G.; Fröhlich, R.; Meyer, O.; Bergander, K. *Helv. Chim. Acta* **1998**, *81*, 1692. (c) Goldman, A. S.; Krogh-Jespersen, K. *J. Am. Chem. Soc.* **1996**, *118*, 12159.

(16) Martínez de Ilarduya, J. M.; Otero, A.; Royo, P. *J. Organomet. Chem.* **1988**, *340*, 187. Gómez, M.; Martínez de Ilarduya, J. M.; Royo, P. *J. Organomet. Chem.* **1989**, *369*, 197.

Table 1. Selected NMR and IR Data of $[(\eta^2\text{-butadiene})\text{Ta}(\text{L})\text{Cp}_2]^+$ Cation Complexes Prepared or Generated in This Study^a

compd	¹ H NMR						¹³ C NMR				IR $\tilde{\nu}(\text{C}=\text{C})$
	1-H/H		2-H	3-H	4-H/H		C1	C2	C3	C4	
2	1.28 ^b	0.88	2.35	6.15	4.91	4.58	24.0	36.1	149.0	104.9	1595
2'	1.60 ^b	1.25	2.11	5.70	4.80	4.64	23.1	35.1	150.9	106.2	c
4a	1.34 ^d	1.11	2.14	4.96	4.68	4.52	23.1	43.9	141.0	111.0	1614
4b	1.83	1.57	2.65	5.40	4.90	4.67	23.1	43.6	142.1	111.5	1613
4c	1.62 ^e	1.58	2.60	5.39	4.90	4.67	23.1	43.6	141.3	111.1	1611
5	1.66 ^f	2.34	3.65	6.11	4.60	4.79	31.8	60.9	147.2	112.2	c
5'	2.21 ^f	2.95	3.02	6.22	4.46	4.58	42.3	50.5	148.8	110.1	c

^a For the structures of the complexes see Schemes 2 and 3; IR spectra are in KBr. ^b NMR in benzene-*d*₆ at 298 K. ^c Not located. ^d NMR in bromobenzene-*d*₅ at 298 K. ^e NMR in dichloromethane-*d*₂ at 298 K. ^f NMR in THF-*d*₈ at 228 K.

Scheme 3

L = *d*₈-THF, all cations with CH₃B(C₆F₅)₃⁻ anion.

THF-*d*₇ slightly off the large THF-*d*₇ solvent resonance in the ¹H (600 MHz) spectrum and the respective THF-*d*₈ features in the ¹³C (150 MHz) NMR spectrum of the sample at 228 K (for details see the Experimental Section), but the complexes **5** and **5'** were not isolated. Therefore, we cannot rigorously rule out that other donor molecules (e.g. the counteranion) have coordinated to the tantalum center in these complexes. Nevertheless, it is quite clear that here we have observed both possible $[(\eta^2\text{-butadiene})\text{Ta}(\text{L})\text{Cp}_2]^+$ complexes with the noncoordinated butadiene vinyl group positioned "inside" (**5**) and "outside" (**5'**) at the front of the bent-metalocene wedge (see Scheme 3). The remaining product (**6**) exhibits only a single Cp resonance (δ 5.54 (¹H); δ 96.9 (¹³C)) in addition to the anion signals. Irradiation of a much more dilute solution of **3** in THF-*d*₈ (at -78 °C, 30 min) resulted in a close to complete conversion of **3** to **6**. Subsequent warming of the sample to room temperature led to a reconversion of **6** to the starting material **3**. We propose that the newly formed complex **6** is $[\text{Cp}_2\text{Ta}(\text{THF-}d_8)_2]^+$.

We then irradiated $[(\text{butadiene})\text{TaCp}_2]^+$ (**3**) in THF-*d*₈ in the presence of an excess of an alkyl isocyanide RN≡C (R = *tert*-butyl or cyclohexyl). In each case the butadiene ligand was cleaved completely with formation of the respective $[\text{Cp}_2\text{Ta}(\text{L})(\text{C}\equiv\text{NR})]^+$ products **7a,b** (L is probably THF-*d*₈) plus free butadiene.

We have then photolyzed **3** in the presence of excess cyclohexyl isocyanide (ca. 4:1 ratio) in THF-*d*₈ at -78 °C. When the photochemically induced butadiene cleavage was complete (ca. 6 h, checked by NMR) the sample was kept for 4 h at 40 °C. This resulted in a subsequent thermally induced exchange of ligands at the tantalocene cation moiety with formation of the complex $[\text{Cp}_2\text{Ta}(\text{C}\equiv\text{N-cyclohexyl})_2]^+\text{MeB}(\text{C}_6\text{F}_5)_3^-$ **8**. Complex **8** was isolated in >50% yield. It shows two prominent IR features ($\tilde{\nu}(\text{C}\equiv\text{NR})$) at 2134 and 2088 cm⁻¹.

Complex **8** shows a single set of ¹H and ¹³C NMR spectra at ambient temperature (dichloromethane-*d*₂, 298 K: ¹H, δ 5.14 (Cp), 3.99 (CH of C₆H₁₁); ¹³C, δ 89.4 (Cp)). There is a single isonitrile carbon resonance at δ 167.5 ppm that is substantially shifted to high δ values relative to free cyclohexyl isocyanide (δ 154.2 ppm (C≡N-)). However, these features correspond to averaged values. Lowering the temperature of the NMR probe rapidly leads to broadening and then splitting of most of the resonances to eventually give rise to the observation of three sets of signals of three isomeric species in a 1:2:1 ratio. A close inspection of the data has revealed that these correspond to the three isomers having the isonitrile functionality at the two cyclohexyl groups in axial and equatorial positions statistically distributed. Thus, the three observed compounds are to be described as the stereoisomers **8**(eq,eq), **8**(eq,ax), and

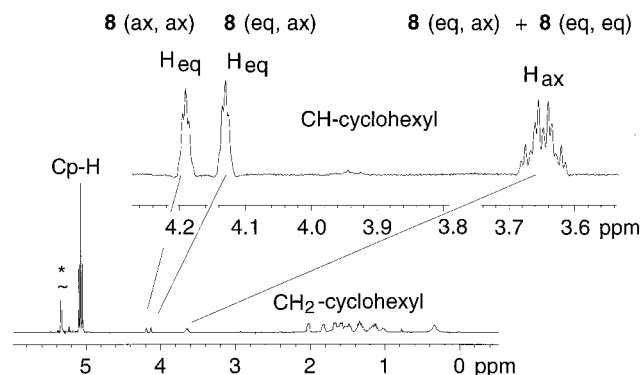


Figure 2. Low-temperature ^1H NMR spectrum (183 K, in dichloromethane- d_2) of the **8(ax,ax)**, **8(eq,ax)**, and **8(eq,eq)** mixture of isomers.

8(ax,ax). Each of them shows a separate $^1\text{H}/^{13}\text{C}$ NMR Cp resonance (δ 5.10/5.07, 5.05 (1:2:1 ratio)/88.8, 88.6, 88.5). The isonitrile (i.e. $\text{C}\equiv\text{N}-$) ^{13}C NMR resonances of all three isomers are clearly distinguished at 150 MHz and 183 K to give rise to four separate signals at δ 166.3, 165.2, 164.3, and 163.1 ppm. The assignment of the three compounds as axially and equatorially substituted $\text{C}\equiv\text{N}$ -cyclohexyl isomers is illustrated by the very characteristic appearance of the low-temperature ^1H NMR spectrum (see Figure 2), in conjunction with a 2D GCOSY experiment. The spectrum shows the 1:2:1 ratio signals of the Cp ligands. The expanded area of the spectrum shows the narrow $\text{C}\equiv\text{N}$ -cyclohexyl CH quintet of **8(ax,ax)** at δ 4.19. The **8(eq,ax)** isomer exhibits a similarly shaped narrow quintet of the CH of the axially substituted cyclohexyl (i.e. exhibiting the methine hydrogen in an equatorial position, which gives rise to the rather small 3J coupling with four gauche methylene hydrogens) at 4.13 ppm. Finally, there are two much wider [N]CH signals closely overlapping (but GCOSY separated) at δ 3.65 ppm. These originate from the equatorially substituted cyclohexyls (methine H axially positioned, resulting in two large and two small 3J couplings) of the isomers **8(eq,ax)** and **8(eq,eq)**, respectively.

Diffusion of pentane vapor into a solution of **8** in tetrahydrofuran gave single crystals that were suited for an X-ray crystal structure analysis. Again, cation and anion are well separated in the crystal (Figure 3). The tantalum center of the cation of **8** is pseudotetrahedrally coordinated by two η^5 -cyclopentadienyls and two κC -cyclohexyl isocyanide ligands.¹² The Cp(centroid)-Ta-Cp(centroid) angle of the bent metallocene **8** is 138.5° . The angle between the σ -ligands (C1-Ta-C8) is $87.3(3)^\circ$. The tantalum-C(isonitrile) bond lengths were determined to be 2.101(9) Å (Ta-C8) and 2.143(8) Å (Ta-C1) (**4c**: 2.118(6) Å), and they are slightly different from each other. Both Ta-C $\equiv\text{N}$ -cyclohexyl units in **8** deviate slightly from linearity. The bond angles of the Ta-C8-N16-C9 unit are $179.4(9)^\circ$ (Ta-C8-N16) and $169.0(13)^\circ$ (C8-N16-C9). The second Ta-isonitrile moiety is slightly more bent at nitrogen (Ta-C1-N15 = $177.4(7)^\circ$, C1-N15-C2 = $163.7(8)^\circ$).

The C8-N16 bond length is 1.149(11) Å, and the C1-N15 distance is 1.143(10) Å. The adjacent N16-C9 (1.440(8) Å) and N15-C2 distances (1.443(8) Å) are also in the expected range.¹³ The structure contains an

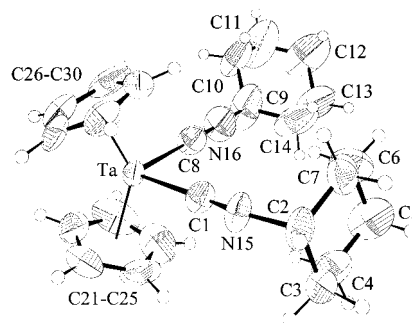


Figure 3. Molecular structure of **8** with nonsystematic atom-numbering scheme. Selected bond lengths (Å) and angles (deg): Ta-C1 = 2.143(8), Ta-C8 = 2.101(9), C1-N15 = 1.143(10), C8-N16 = 1.149(11), N15-C2 = 1.443(8), N16-C9 = 1.440(8); C1-Ta-C8 = $87.3(3)^\circ$, Ta-C1-N15 = $177.4(7)^\circ$, Ta-C8-N16 = $179.4(9)^\circ$, C1-N15-C2 = $163.7(8)^\circ$, C8-N16-C9 = $169.0(13)^\circ$.

Table 2. Selected Structural and IR Data for Metallocene Alkyl Isocyanide Adducts from the Literature for a Comparison^a

compd	M-C $\equiv\text{N}^b$	C $\equiv\text{N}$ -R ^b	C $\equiv\text{N}^c$	$\tilde{\nu}(\text{C}\equiv\text{NR})^d$	ref
9	174.7(3)	173.1(3)	1.133(2)	2310	15a
10	<i>e</i>	<i>e</i>	<i>e</i>	2247	17
11	178.4(2)	178.9(3)	1.145(4)	2209	7
12	172.5(5)	176.6(6)	1.154(6)	2195	18
13	<i>e</i>	<i>e</i>	<i>e</i>	2090	16
14	<i>e</i>	<i>e</i>	<i>e</i>	2180	16
15	179(1)	175(2)	1.19(2)	2050 ^f 2070 ^f	19
16	<i>g</i>	172.0(13) 167.3(13)	1.143(18) 1.166(18)	2137 2102	20
17	178.5(15) 179.4(16)	176.6(9) 173.4(16)	1.122(6) 1.133(6)	2250 2240	21
4c	177.2(5)	174.0(8)	1.152(6)	2174	this work
8	179.4(9) 177.4(7)	169.0(13) 163.7(8)	1.149(11) 1.143(10)	2134 2088	this work
18	<i>e</i>	<i>e</i>	<i>e</i>	1770	19
19	173.1(3)	139.5(4)	1.193(4)	1852 ^h	22

^a Structures of the compounds **9–19** are depicted in Chart 1. ^b Bond angles in deg. ^c Bond lengths in Å. ^d In KBr; $\tilde{\nu}$ in cm^{-1} . ^e Not determined. ^f C $\equiv\text{N}$ (R) and C $\equiv\text{N}$ bands. ^g Not listed. ^h In pentane.

axially substituted cyclohexyl ring at N15, whereas the C9-C14 cyclohexyl ring at N16 is conformationally disordered (for details see the Experimental Section). A comparison with relevant structural data from the literature (see Table 2 and Chart 1) shows that the Ta-C $\equiv\text{N}$ C₆H₁₁ bonding features are in a very typical range, close to values that have been observed for a variety of related para- and diamagnetic four-coordinate, pseudotetrahedral vanadocene or niobocene complexes.

These systems show linear, or at the most slightly bent, M-C $\equiv\text{N}$ -R units, and they are characterized by a shifting of the $\tilde{\nu}(\text{C}\equiv\text{NR})$ IR bands to *higher* wavenumbers relative to the free alkyl isocyanide ligand. The structural features of **8** are remarkably similar to those of the *ansa*-vanadocene cation **16**, recently described by Brintzinger et al. (see Table 2). In contrast, three-coordinate Cp₂M-C $\equiv\text{NR}$ systems such as **18** and **19** show the strong bending at nitrogen and substantial lowering of the isonitrile IR band that is expected for a situation characterized by strong metal to ligand back-bonding. The slight bending at nitrogen in **8** is probably not caused by an onsetting back-bonding effect but seems to have other reasons.

We conclude from these experimental findings that metal to ligand back-bonding effects seem to be not of

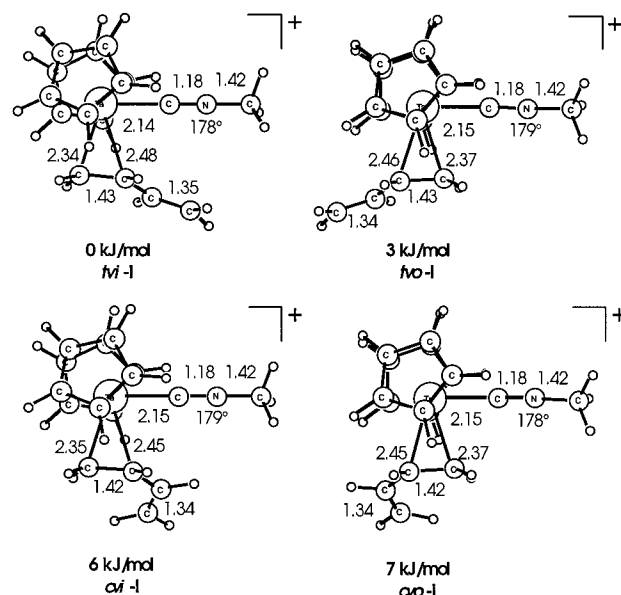
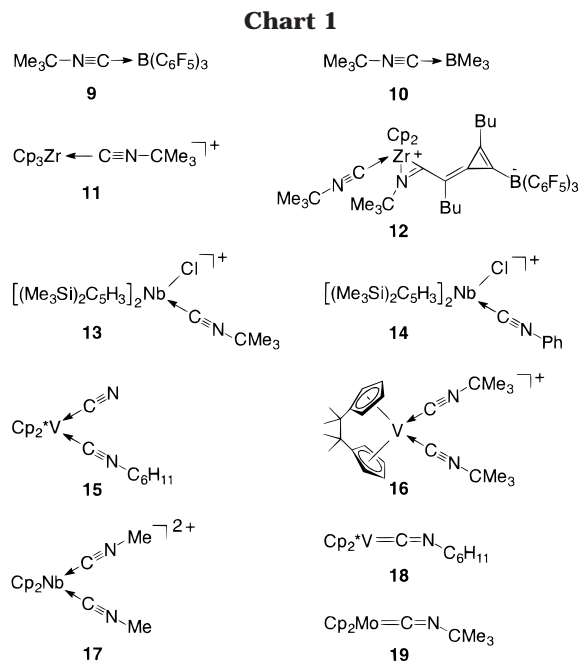


Figure 4. Optimized geometries and relative energies for various isomers of $[(\eta^2\text{-butadiene})(\text{CH}_3\text{N}=\text{C})\text{TaCp}_2]^+$ (**I**).

major importance for the description of the distorted tetrahedral (isonitrile)(L)tantalocene cation complexes (**4**, **8**) investigated in this study. It appears that the $\text{Ta}-\text{C} \equiv \text{NR}$ coordination is probably dominated by electrostatic effects¹⁵ and thus is very similar to the general bonding situation that was previously observed and characterized for a variety of d^0 -configured $[\text{M}]-\text{C} \equiv \text{NR}$ (or $\text{C} \equiv \text{O}$ and $\text{N} \equiv \text{CR}$) type complexes.^{7,10}

Bonding of Tantalocene Cation with Alkyl Isonitrile: Quantum-Chemical Calculations. To further investigate the bonding of isocyanides with cationic metallocene fragments, as manifested in compounds **4** and **8**, we performed density functional calculations²³ on a set of representative model compounds. We wanted to gain a deeper understanding of the interplay between electrostatic effects and π back-donation in ligand to metal bonding and to explore the energetics of different structural isomers which one might encounter.

In connection with the latter problem, the structures of four different isomers of $[(\eta^2\text{-butadiene})(\text{CH}_3\text{N}=\text{C})\text{TaCp}_2]^+$ (**I**) have been optimized. As indicated in the previous sections, there exist several possibilities for the structure of $[(\eta^2\text{-butadiene})\text{Ta}(\text{L})\text{Cp}_2]^+$, in particular concerning the orientation of the butadiene ligand. The results of the calculations are presented in Figure 4. In the most stable isomer, **tv-i** (i.e., *trans-vinyl-inside*), the butadiene ligand possesses an *s-trans* orientation and is coordinated to the isocyanide in "vinyl-inside" fashion. Not only this arrangement but also other main geometric features are in accord with the crystal struc-

ture of **4c**. The isocyanide unit is almost ideally linear, and the η^2 -butadiene ligand is bonded to the metal center in an asymmetric fashion, the terminal C-atom forming the shorter Ta-C bond. The calculated energetic differences between the four isomers, however, are small; the second lowest structure **tvo-i** is only 3 kJ/mol higher in energy and represents the "vinyl-outside" isomer. The two *s-cis*-butadiene structures, **cvi-i** and **cvo-i**, lie 6 and 7 kJ/mol higher in energy, respectively, again with a slight preference for "vinyl-inside" coordination.

The substantially elongated coordinated double bond indicates that the d^2 transition-metal fragment is indeed capable of some back-bonding. There is, however, no structural evidence that back-bonding to the isocyanide ligand also takes place. One would expect an elongation of the $(\text{R})\text{N} \equiv \text{C}$ triple bond and bending of the central nitrogen atom of the CNR ligand.¹⁶ In all four isomers the geometry of the isocyanide does not change under coordination and is essentially the same as calculated for the free ligand ($d_{\text{MeN}=\text{C}} = 1.18 \text{ \AA}$ and $d_{\text{Me}-\text{NC}} = 1.42 \text{ \AA}$).

Changes in the coordination geometry of the $\text{RN} \equiv \text{C}$ ligand are found in complexes of the type $[(\text{RNC})_2\text{-TaCp}_2]^+$, in which the isocyanide ligand does not compete with an olefinic double bond for back-bonding. The optimized geometry for $[(\text{MeNC})_2\text{TaCp}_2]^+$ (**II**) is displayed in Figure 5. The two isocyanide ligands are of different coordination geometries, one being almost linear and the other being bent at the central N atom by 17° , and they show slightly different ligand to metal bond distances. These geometric parameters are in good agreement with the structural features of the related compound **8**. We also carried out a calculation in which identical local geometry of the isocyanides was enforced by applying a C_2 symmetry constraint. The resulting structure, C_2 -**II**, is of virtually the same energy as **II** and again shows CNMe units which deviate from linearity by 14° (Figure 5).

The Ta-CNR separation is calculated to be somewhat smaller in **II** than in **I**, which might be indicative of a

(17) Casanova, J.; Schuster, R. E. *Tetrahedron Lett.* **1964**, 405.

(18) Ahlers, W.; Erker, G.; Fröhlich, R.; Peuchert, U. *J. Organomet. Chem.* **1999**, 578, 115.

(19) Gambarotta, S.; Floriani, C.; Chiesi-Villa, A.; Guastini, C. *Inorg. Chem.* **1984**, 23, 1739.

(20) Dorer, B.; Prosenc, M.-H.; Rief, U.; Brintzinger, H.-H. *Collect. Czech. Chem. Commun.* **1997**, 62, 265.

(21) Carrondo, M. A. F. de C. T.; Morais, J.; Romão, C. C.; Romão, M. J.; Veiros, L. F. *Polyhedron* **1993**, 12, 765.

(22) Martins, A. M.; Calhorda, M. J.; Romão, C. C.; Völkl, C.; Kiprof, P.; Filippou, A. C. *J. Organomet. Chem.* **1992**, 423, 367.

(23) (a) Kohn, W.; Becke, A. D.; Parr, R. G. *J. Phys. Chem.* **1996**, 100, 12974. (b) Baerends, E. J.; Gritsenko, O. V. *J. Phys. Chem. A* **1997**, 101, 5383.

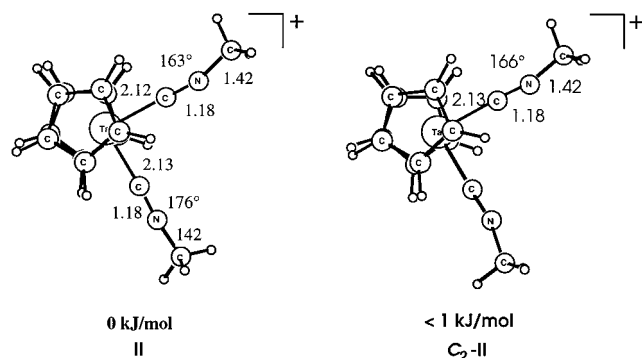


Figure 5. Computed structure of $[(\text{CH}_3\text{N}=\text{C})_2\text{TaCp}_2]^+$ (**II**).

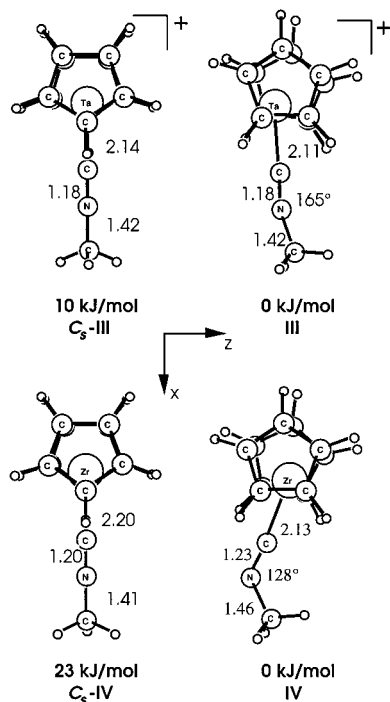


Figure 6. $[(\text{CH}_3\text{N}=\text{C})\text{MCp}_2]^+$ complexes (**III**, $\text{M} = \text{Ta}$, $n = 1$; **IV**, $\text{M} = \text{Zr}$, $n = 0$) with linear and bent isonitrile ligands.

small increase in metal to ligand bond strength, presumably because of enhanced back-bonding. This also serves to explain the slight bending of the coordinated isonitrile ligand. To address the question of what extent back-bonding to the isonitrile ligand is actually of importance, the model compound $[(\text{MeNC})\text{TaCp}_2]^+$ (**III**) and the related isoelectronic, but neutral, complex $[(\text{MeNC})\text{ZrCp}_2]$ (**IV**) have been investigated.

We first look at the complexes with a linearly coordinated isonitrile ligand, which have been restricted to C_s symmetry in such a way that the mirror plane bisects the two cyclopentadienyl ligands of the MCp_2 unit. The optimized geometries for C_s -**III** and C_s -**IV** are displayed in Figure 6. It is noticeable that in the neutral complex C_s -**IV** the $\text{C}\equiv\text{N}$ bond is elongated by 0.02 Å, compared to C_s -**III** or the free ligand.

A detailed analysis of the bond between the metallocene fragment M and the isonitrile L clarifies the nature of the $\text{M}-\text{L}$ interaction. The energy BE associated with the bond-forming reaction $\text{M} + \text{L} \rightarrow \text{M}-\text{L}$ can essentially be broken down²⁴ into contributions due to Pauli repulsion ΔE_{Pauli} , the electrostatic term ΔE_{elstat} ,

Table 3. Bond Analysis^a of $[(\text{CH}_3\text{N}=\text{C})\text{MCp}_2]^+$ Complexes (III**, $\text{M} = \text{Ta}$, $n = 1$; **IV**, $\text{M} = \text{Zr}$, $n = 0$) with Linear-Coordinated Isonitrile**

	C_s - III	C_s - IV		C_s - III	C_s - IV
ΔE_{Pauli}	468	363	$\Delta E_{\text{int}}(\text{A}')$	-90	-114
ΔE_{elstat}	-451	-305	BE	295	178
$\Delta E_{\text{int}}(\text{A}'')$	-222	-122			

^a In kJ/mol.

and orbital interactions ΔE_{int} :

$$\text{BE} = -[\Delta E_{\text{Pauli}} + \Delta E_{\text{elstat}} + \Delta E_{\text{int}}(\text{A}') + \Delta E_{\text{int}}(\text{A}'')] \quad (2)$$

In eq 2, ΔE_{int} is further split into contributions from different irreducible representations according to C_s symmetry. The orbital structure of metallocenes is well understood,^{12,25} and the three important frontier orbitals all lie in the major coordination plane at the front sector of the metallocene wedge (the xz plane as defined in Figure 6). The orbital responsible for back-bonding will be mainly $\text{M } d_{xz}$ based (corresponding to b_2 in C_{2v} symmetry), and is antisymmetric with respect to the xy mirror plane. Thus, the term $\Delta E_{\text{int}}(\text{A}'')$ will represent the main contributions to π back-bonding. The results of the analysis are collected in Table 3. For the cationic tantalocene complex C_s -**III**, we find some contribution due to π back-bonding, which, however, is more than 2 times smaller than the σ component $\Delta E_{\text{int}}(\text{A}')$. Furthermore, we have a strong electrostatic component, which almost compensates for all the repulsive interaction. In contrast, for the neutral zirconocene complex, the σ and π contributions are of almost equal importance and the absolute value of the electrostatic interaction now is smaller than that of the Pauli repulsion. This bonding situation is similar to that encountered in classical π back-bonding complexes, where the π component is often stronger than the σ component. An analysis of the first bond dissociation energy in $\text{W}(\text{CO})_6$, for example, results in values of 150 and 173 kJ/mol for ΔE_{G} and ΔE_{T} , respectively.²⁶

When the symmetry constraint is lifted, both structures C_s -**III** and C_s -**IV** undergo a stabilizing bending of the isonitrile unit (Figure 6). The changes in CNMe coordination geometry when going from C_s -**III** to **III** are similar to those found when comparing **I** and **II** or **4** and **8**. The metal to ligand bond shortens by about 0.02 Å, and the isonitrile ligands bend by about 15°, but no significant changes in $\text{C}\equiv\text{N}$ bond length are noticed. For **IV**, the ligand distortion is more drastic. The angle at the central N atom of 128° approaches the sp^2 value, and the $\text{C}\equiv\text{N}$ bond elongates by 0.03 Å. The coordination geometry of the hypothetical $16e^-$ complex $[(\text{MeNC})\text{ZrCp}_2]$ is strongly reminiscent of that observed for $[(\text{tBuNC})\text{MoCp}_2]$.²²

The bonding analysis becomes less instructive for complexes **III** and **IV**, mostly because the different interaction terms can no longer be differentiated by symmetry. One can, however, assess the importance of the π component by means of a Mulliken population

(24) Ziegler, T. *NATO ASI Ser.* **1992**, C378, 367. See ref 15a,b for a more detailed description and further references.

(25) Green, J. C. *Chem. Soc. Rev.* **1998**, 27, 263.

(26) Ehlers, A. W.; Ruiz-Morales, Y.; Baerends, E. J.; Ziegler, T. *Inorg. Chem.* **1997**, 36, 5031.

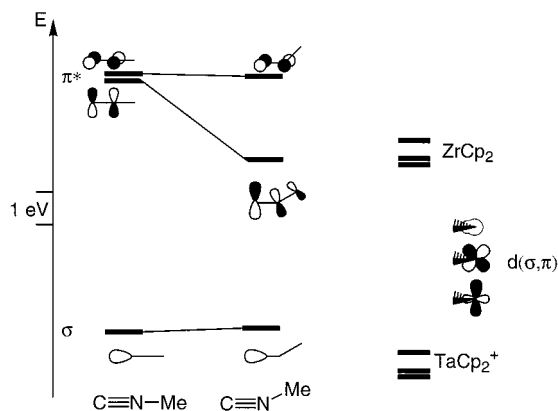


Figure 7. Frontier orbital diagram for isonitrile and $[MCp_2]^{n+}$ fragments ($M = Ta, n = 1$; $M = Zr, n = 0$).

analysis. The total population of the formerly empty virtual orbitals of the isonitrile ligand in the final molecule serves as a measure for back-bonding. For both systems, the value so defined increases under bending and goes from 0.36 to 0.42 au for C_s -**III** \rightarrow **III** and from 0.48 au to 0.73 au for C_s -**IV** \rightarrow **IV**. Although the absolute values should not be taken too seriously, the general trend becomes clear. Back-bonding increases under ligand distortion, to a small amount for the cationic tantalocene and to a major extent for the neutral zirconocene.

The main features of the transition-metal isonitrile bond are well-understood,²⁷ and the origin of the bending distortion has been analyzed.²⁸ The degeneracy of the π^* orbitals is lifted, and one of these orbitals is considerably lowered in energy. This in turn leads to a more effective back-bonding interaction with a transition-metal center, and this additional stabilization of the transition metal to ligand bond outweighs the destabilization of the ligand framework. In contrast to the π -acceptor capability of the isonitrile ligand, the σ -donor ability changes little with the degree of bending. An illustrative orbital energy diagram for CN-Me and the $ZrCp_2$ and $[TaCp_2]^+$ fragments is presented in Figure 7. The valence d-orbital set for the Ta fragment lies about 6 eV lower in energy compared to Zr, which is mainly caused by the positive charge on the metal center. Bending of the isonitrile only slightly enhances the interaction of the orbitals involved in π bonding, whereas for the Zr a strong bending results in a good match in energy between the ligand π^* -acceptor and the metal $d(\pi)$ -donor orbital. The balance between stabilization due to enhanced back-bonding and destabilization due to distortion of the ligand framework thus results in a small bending for **III** but in a large bending for **IV**. On the other hand, the σ -donor orbital of the isonitrile is close in energy to the d set of **IV** but is well-separated from that of **III**. We can expect a much stronger donor interaction in case of $[TaCp_2]^+$, which is in accord with our bond analysis as presented in Table 3.

To further illustrate the importance of the electrostatic component for the transition-metal-isonitrile bond, we compared complex C_s -**III** with the model nitrile adduct $[(MeCN)TaCp_2]^+$ (C_s -**V**). We introduce the

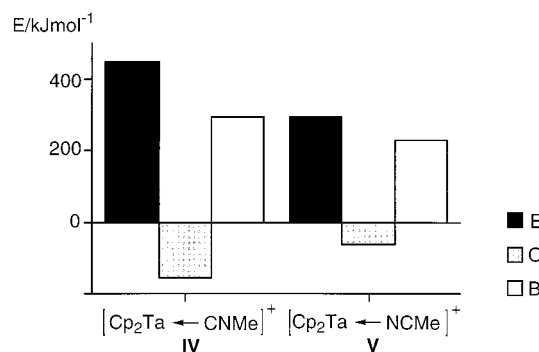


Figure 8. Energy decomposition of the bond energy (B) of the M-L bond according to orbital terms and electrostatic terms. The negative values of ΔE_{orb} (O) and ΔE_{elstat} (E) are shown, so that in any case positive energy values indicate stabilization, and vice versa.

orbital term ΔE_{orb} , in which electronic interaction and Pauli repulsion are combined,^{15a,b} and write the bond energy BE as

$$BE = -[\Delta E_{orb} + \Delta E_{elstat}] \quad (3)$$

The results of this analysis are shown in Figure 8. As we have found in previous studies,^{15a,b} the isonitrile ligand undergoes a very strong electrostatic interaction with the cationic metal fragment, which stabilizes the metal-ligand bond by 65 kJ/mol, compared to the acetonitrile ligand. This electrostatic stabilization might be one of the reasons isonitrile complexes such as **4** are isolable and do not readily undergo insertion reactions as do other unsaturated reagents, such as nitriles and ketones.

In summary, the computational study supports the notation that back-donation does not represent a major bonding interaction between isonitriles and the tantalocene cation, especially if the isonitrile has to compete with other strong π acceptors for electron density from the metal center as in **4**. Here, the bonding is dominated by electrostatic effects, which manifest themselves in a $\tilde{\nu}[C\equiv N]$ band which is shifted to higher wavenumbers from the value of the free ligand.¹⁵ In cases where isonitriles are the only π acceptors present, as in the case of **8**, the amount of back-bonding increases and induces a bent of the isonitrile ligand. This counters the changes in the shift of the $\tilde{\nu}[C\equiv N]$ band due to electrostatics, and as a consequence $\tilde{\nu}[C\equiv N]$ in **8** is shifted to lower wavenumbers by 30–80 cm^{-1} compared to **4**.

Experimental Section

All reactions were carried out under an inert atmosphere (argon), using Schlenk-type glassware, or in a glovebox. Solvents, including deuterated solvents, were dried and distilled under argon prior to use. $[(s\text{-}trans\text{-}\eta^4\text{-butadiene})TaCp_2]^+CH_3B(C_6F_5)_3^-$ (**3**) was prepared as recently described by us in the literature.⁴ See also ref 4 for additional general information.

Reaction of 3 with tert-Butyl Isocyanide. Preparation of (η^2 -Butadiene)(κ -C-tert-butyl isocyanide)bis(η^3 -cyclopentadienyl)tantalum Methyltris(pentafluorophenyl)borate (4a**).** tert-Butyl isocyanide (41.0 mg, 493 μ mol) was added to a solution of 400 mg (452 μ mol) of **3** in 10 mL of bromobenzene. The mixture was stirred at 45 $^\circ$ C for 4 h. At room temperature 10 mL of pentane was added to precipitate the product. The supernatant liquid was removed and the

(27) Sarapu, A. C.; Fenske, R. F. *Inorg. Chem.* **1975**, *14*, 247.

(28) Howell, J. A. S.; Saillard, J.-Y.; Le Beuze, A.; Jaouen, G. *J. Chem. Soc., Dalton Trans.* **1982**, 2533.

crude product dissolved in 5 mL of dichloromethane. The product was precipitated again by the addition of pentane (10 mL). The solvent was decanted off and the residue dissolved in 3 mL of pentane. Diffusion of pentane vapor into this solution furnished the product **4c** as a red solid: yield 302 mg (69%); mp 131 °C. Anal. Calcd for $C_{38}H_{28}NBF_{15}Ta$ (975.4): C, 46.80; H, 2.89; N, 1.44. Found: C, 46.14; H, 3.21; N, 1.69. IR (KBr): $\tilde{\nu}$ 3126 (w), 2980 (w), 2957 (w), 2164 (s), 1641 (m), 1614 (w), 1511 (vs), 1458 (vs), 1372 (w), 1266 (m), 1188 (m), 1087 (vs), 1010–940 (br m), 840 (s), 802 (w) cm^{-1} . 1H NMR (bromobenzene- d_5 , 599.8 MHz, 298 K): δ 4.96 (ptd, $^3J_{HH} = 16.6$ Hz, 9.8 Hz, 1H, 3-H), 4.69 (s, 5H, Cp H), 4.68 (d, $^3J_{HH} = 16.6$ Hz, 1H, 4-H), 4.67 (s, 5H, Cp H), 4.52 (dd, $^3J_{HH} = 9.8$ Hz, $^2J_{HH} = 1$ Hz, 1H, 4-H), 2.13 (m, 1H, 2-H), 1.34 (dd, $^3J_{HH} = 9.9$ Hz, $^2J_{HH} = 5.4$ Hz, 1H, 1-H), 1.22 (s, 9H, CM_e_3), 1.11–1.08 (m, 4H, 1-H and $Me-B(C_6F_5)_3$) ppm. 1D TOCSY NMR (bromobenzene- d_5 , 599.8 MHz, 298 K): irradiation at δ 2.14 (2H) ppm; response at δ 4.96 (3-H), 4.68 (4-H), 4.52 (4-H), 1.34 (1-H), 1.09 (1-H) ppm. ^{13}C NMR (bromobenzene- d_5 , 150.8 MHz, 298 K): δ 156.9 (C5), 148.8 (d, $^1J_{CF} = 232$ Hz, $o-B(C_6F_5)_3$), 141.0 (C3), 137.8 (d, $^1J_{CF} = 233$ Hz, $p-B(C_6F_5)_3$), 136.7 (d, $^1J_{CF} = 233$ Hz, $m-B(C_6F_5)_3$), 111.0 (C4), 96.8, 96.5 (each C Cp), 59.7 (CM_e_3), 43.9 (C2), 30.1 (CH_3), 23.4 (C1), 11.1 ($Me-B(C_6F_5)_3$) ppm; ipso C of C_6F_5 not observed.

Reaction of 3 with *n*-Butyl Isocyanide. Preparation of (η^2 -Butadiene)(κ -*n*-butyl isocyanide)bis(η^5 -cyclopentadienyl)tantalum Methyltris(pentafluorophenyl)borate (4b**).** Analogously as described above, 35.9 mg (430 μ mol) of $n-C_4H_9N\equiv C$ was reacted with 350 mg (390 μ mol) of **3** in 10 mL of bromobenzene at 45 °C for 3 h. Workup with dichloromethane/pentane analogously as described above gave 289 mg (76%) of **4b** as red crystals, mp 143 °C. Anal. Calcd for $C_{38}H_{28}NBF_{15}Ta$ (975.4): C, 46.80; H, 2.89; N, 1.44. Found: C, 46.21; H, 3.20; N, 1.76. IR (KBr): $\tilde{\nu}$ 3119 (w), 2963 (m), 2938 (m), 2185 (s), 1641 (m), 1613 (m), 1510 (vs), 1459 (vs), 1381 (vw), 1263 (s), 1088 (vs), 1002–948 (br s), 842 (vs), 834 (vs), 660 (w), 605 (w) cm^{-1} . 1H NMR (dichloromethane- d_2 , 599.8 MHz, 298 K): δ 5.40 (ptd, $^3J_{HH} = 16.7$ Hz, 9.8 Hz, 1H, 3-H), 5.30/5.15 (s, each 5H, Cp H), 4.90 (ddd, $^3J_{HH} = 16.7$ Hz, $^2J_{HH} = 1.7$ Hz, $^4J_{HH} = 0.9$ Hz, 1H, 4-H), 4.67 (ddd, $^3J_{HH} = 9.8$ Hz, $^2J_{HH} = 1.7$ Hz, $^4J_{HH} = 0.4$ Hz, 1H, 4-H), 4.11–4.06 (m, 2H, [N]– CH_2 –), 2.68–2.62 (m, 1H, 2-H), 1.88–1.83 (m, 2H, CH_2), 1.83 (dd, $^3J_{HH} = 10.2$ Hz, $^2J_{HH} = 5.4$ Hz, 1H, 1-H), 1.57 (dd, $^3J_{HH} = 12.8$ Hz, $^2J_{HH} = 5.4$ Hz, 1H, 1-H), 1.52–1.46 (m, 2H, CH_2), 1.03 (t, $^3J_{HH} = 7.4$ Hz, 3H, CH_3), 0.50 (br s, 3H, $Me-B(C_6F_5)_3$) ppm. NOE NMR (dichloromethane- d_2 , 599.8 MHz, 298 K): (1) irradiated at δ 1.57 (1-H), response at δ 1.83 (1-H); (2) irradiated at δ 1.83 (1-H), response at 2.65 (2-H), 1.57 (1-H); (3) irradiated at δ 2.65 (2-H), response at 4.90 (4-H), 1.83 (1-H); (4) irradiated at δ 4.67 (4-H), response at 5.40 (3-H), 4.90 (4-H); (5) irradiated at δ 4.90 (4-H), response at 4.67 (4-H), 2.65 (2-H); (6) irradiated at δ 5.40 (3-H), response at 4.67 (4-H). 1H NMR (bromobenzene- d_5 , 599.8 MHz, 298 K): δ 5.03 (ptd, $^3J_{HH} = 16.6$ Hz, 9.8 Hz, 1H, 3-H), 4.70 (s, 5H, Cp H), 4.69 (ddd, $^3J_{HH} = 16.6$ Hz, $^2J_{HH} = 1.6$ Hz, $^4J_{HH} = 0.9$ Hz, 1H, 4-H), 4.64 (s, 5H, Cp H), 4.52 (pdd, $^3J_{HH} = 9.8$ Hz, $^2J_{HH} = 1.7$ Hz, 1H, 4-H), 3.68–3.60 (m, 2H, [N]– CH_2), 2.25–2.20 (m, 1H, 2-H), 1.48–1.43 (m, 2H, CH_2), 1.33 (dd, $^3J_{HH} = 9.9$ Hz, $^2J_{HH} = 5.4$ Hz, 1H, 1-H), 1.19–1.13 (m, 2H, CH_2), 1.10 (br s, 3H, $Me-B(C_6F_5)_3$), 1.09 (dd, $^3J_{HH} = 12.9$ Hz, $^2J_{HH} = 5.4$ Hz, 1H, 1-H), 0.79 (t, $^3J_{HH} = 7.4$ Hz, 3H, CH_3) ppm. 1D TOCSY NMR (bromobenzene- d_5 , 599.8 MHz, 298 K): irradiated at δ 2.22 (2H) ppm, response at δ 5.03 (3-H), 4.69 (4-H), 4.52 (4-H), 1.33 (1-H), 1.09 (1-H) ppm. ^{13}C NMR (bromobenzene- d_5 , 150.8 MHz, 298 K): δ 156.6 (C5), 148.8 (d, $^1J_{CF} = 233$ Hz, $o-B(C_6F_5)_3$), 142.1 (C3), 137.7 (d, $^1J_{CF} = 233$ Hz, $p-B(C_6F_5)_3$), 136.7 (d, $^1J_{CF} = 234$ Hz, $m-B(C_6F_5)_3$), 111.5 (C4), 96.8, 96.5 (each C Cp), 46.4 ([N]– CH_2), 43.6 (C2), 31.3 (CH_2), 23.9 (C1), 19.8 (CH_2), 13.1 (CH_3), 11.1 ($Me-B(C_6F_5)_3$) ppm; ipso C of C_6F_5 not observed.

X-ray crystal structure analysis of **4b**: formula $C_{38}H_{28}NBF_{15}$ -

Ta, $M_r = 975.37$, $0.40 \times 0.20 \times 0.10$ mm, $a = 12.622(1)$ Å, $b = 14.559(1)$ Å, $c = 19.111(1)$ Å, $V = 3511.9(4)$ Å³, $\rho_{calcd} = 1.845$ g cm^{-3} , $\mu = 32.41$ cm^{-1} , absorption correction via SORTAV ($0.357 \leq T \leq 0.738$), $Z = 4$, orthorhombic, space group $P2_12_12_1$ (No. 19), $\lambda = 0.71073$ Å, $T = 198$ K, ω and φ scans, 21 190 reflections collected ($\pm h, \pm k, \pm l$), $(\sin \theta)/\lambda = 0.67$ Å⁻¹, 8460 independent and 7729 observed reflections ($I \geq 2 \sigma(I)$), 507 refined parameters, $R = 0.039$, $R_w = 0.091$, maximum residual electron density 2.44 (–1.14) e Å⁻³ close to Ta, hydrogens calculated and refined riding. The anisotropic thermal parameters indicates large movements or positional disorder, especially in the *n*-butyl–N≡C and the butadiene units. Refinement with split positions was not possible; therefore the *n*-butyl group was refined with the SADI restraint. The resulting large standard deviations of the geometrical data do not permit a discussion of this or a comparison with other structures. Nevertheless, the analysis confirms the chemical composition of the compound.

Reaction of 3 with Cyclohexyl Isocyanide. Preparation of (η^2 -Butadiene)(κ -C-cyclohexyl isocyanide)bis(η^5 -cyclopentadienyl)tantalum Methyltris(pentafluorophenyl)borate (4c**).** Treatment of 400 mg (450 μ mol) of **3** with 53.8 mg (490 μ mol) of cyclohexyl isocyanide in 10 mL of bromobenzene at 45 °C for 3 h and subsequent workup analogously as described above gave 334 mg (74%) of **4c** as red crystals that were suited for X-ray crystal structure analysis; mp 141 °C. Anal. Calcd for $C_{40}H_{30}NBF_{15}Ta$ (1001.4): C, 47.99; H, 3.02; N, 1.41. Found: C, 47.82; H, 3.13; N, 1.60. IR (KBr): $\tilde{\nu}$ 3123 (vw), 2942 (m), 2863 (w), 2174 (s), 1642 (m), 1611 (w), 1510 (vs), 1458 (vs), 1372 (w), 1365 (w), 1264 (m), 1088 (vs), 1080 (s), 1003–946 (br m), 841 (s), 831 (m), 802 (w) cm^{-1} . 1H NMR (dichloromethane- d_2 , 599.8 MHz, 298 K): δ 5.39 (ptd, $^3J_{HH} = 16.6$ Hz, 9.8 Hz, 1H, 3-H), 5.29/5.27 (s, each 5H, Cp H), 4.90 (ddd, $^3J_{HH} = 16.6$ Hz, $^2J_{HH} = 1.6$ Hz, $^4J_{HH} = 0.9$ Hz, 1H, 4-H), 4.67 (ddd, $^3J_{HH} = 9.8$ Hz, $^2J_{HH} = 1.6$ Hz, $^4J_{HH} = 0.4$ Hz, 1H, 4-H), 4.19 (m, 1H, [N]–CH), 2.62–2.58 (m, 1H, 2-H), 2.15–2.10 (m, 4H, CH_2), 1.82 (dd, $^3J_{HH} = 10.1$ Hz, $^2J_{HH} = 5.5$ Hz, 1H, 1-H), 1.79–1.70 (m, 6H, CH_2), 1.58 (dd, $^3J_{HH} = 12.9$ Hz, $^2J_{HH} = 5.5$ Hz, 1H, 1-H), 1.74–1.38 (m, 2H, CH_2), 0.50 (br s, 3H, $Me-B(C_6F_5)_3$). 1D TOCSY NMR (dichloromethane- d_2 , 599.8 MHz, 298 K): irradiation at δ 2.60 (2-H), response at δ 5.39 (3-H), 4.90 (4-H), 4.67 (4-H), 1.82 (1-H), 1.58 (1H) ppm. ^{13}C NMR (bromobenzene- d_5 , 150.8 MHz, 298 K): δ 156.5 (C5), 148.7 (d, $^1J_{CF} = 230$ Hz, $o-B(C_6F_5)_3$), 141.3 (C3), 137.6 (d, $^1J_{CF} = 234$ Hz, $p-B(C_6F_5)_3$), 136.6 (d, $^1J_{CF} = 233$ Hz, $m-B(C_6F_5)_3$), 111.1 (C4), 96.7, 96.4 (each C Cp), 56.8 ([N]–CH), 43.6 (C2), 33.0, 32.8, 24.4, 23.4 (CH_2), 23.3 (C1), 10.8 ($Me-B(C_6F_5)_3$) ppm; ipso C of C_6F_5 not observed. ESI MS (dichloromethane- d_2): cation, m/z 474 (<1%), 420 (70%), 338 (100%), 311 (68%).

X-ray crystal structure analysis of **4c**: formula $C_{40}H_{30}NBF_{15}Ta$, $M_r = 1001.41$, $0.30 \times 0.25 \times 0.10$ mm, $a = 12.667(1)$ Å, $b = 14.864(1)$ Å, $c = 19.263(1)$ Å, $V = 3626.9(4)$ Å³, $\rho_{calcd} = 1.834$ g cm^{-3} , $\mu = 31.41$ cm^{-1} , absorption correction via SORTAV ($0.453 \leq T \leq 0.744$), $Z = 4$, orthorhombic, space group $P2_12_12_1$ (No. 19), $\lambda = 0.71073$ Å, $T = 198$ K, ω and φ scans, 31 595 reflections collected ($\pm h, \pm k, \pm l$), $(\sin \theta)/\lambda = 0.71$ Å⁻¹, 10 530 independent and 8094 observed reflections ($I \geq 2 \sigma(I)$), 525 refined parameters, $R = 0.049$, $R_w = 0.071$, maximum residual electron density 1.57 (–1.06) e Å⁻³ close to Ta, hydrogens calculated and refined riding. The structure could only be refined with the assumption of a racemic twin; with this crystal the resulting ratio was [0.45(1)]:[0.55(1)]. We collected data sets from different attempts on different instruments; all of them showed this effect, and the resulting ratios were always about 0.50:0.50.

Photolysis of 3 in THF- d_8 . Generation of the Complexes 5, 5', and 6. Two NMR experiments were carried out. In the first, a solution of 80.0 mg (89.6 μ mol) of **3** in 0.8 mL of THF- d_8 was photolyzed (Philips HPK 125 lamp, Pyrex filter) at –78 °C for 1 h. NMR measurement at –45 °C revealed the

presence of a mixture of the complexes **3**, **5**, **5'**, and **6** in a 55:10:5:30 ratio. In a second NMR experiment a less concentrated solution, which contained 20 mg (22.4 μmol) of **3** in 0.8 mL of THF-*d*₆, was irradiated under similar conditions for 30 min. In this case an almost quantitative generation of **6** and noncoordinated butadiene was observed. These products were not isolated but only characterized by NMR spectroscopy. Data for **5** are as follows. ¹H NMR (THF-*d*₆, 599.8 MHz, 228 K): δ 6.11 (ptd, ³J_{HH} = 9.7 Hz, 17.0 Hz, 1H, 3-H), 5.90, 5.75 (s, each 5H, Cp H), 4.79 (d, ³J_{HH} = 17.0 Hz, 1H, 4-H'), 4.60 (d, ³J_{HH} = 9.7 Hz, 1H, 4-H), 3.65 (m, 1H, 2-H), 2.84 (dd, ³J_{HH} = 10.2 Hz, ²J_{HH} = 6.2 Hz, 1H, 1-H'), 1.66 (dd, ³J_{HH} = 11.6 Hz, ²J_{HH} = 6.2 Hz, 1H, 1-H), 0.45 (br s, 3H, *Me*-B(C₆F₅)₃) ppm. 1D TOCSY NMR (THF-*d*₆, 599.8 MHz, 228 K): irradiation at δ 4.79 (4-H'), response at δ 6.11 (3-H), 4.60 (4-H), 3.65 (2-H), 2.84 (1-H'), 1.66 (1-H) ppm. ¹³C NMR (THF-*d*₆, 150.8 MHz, 228 K): δ 149.0 (d, ¹J_{CF} = 235 Hz, *o*-B(C₆F₅)₃), 147.3 (gated: d, ¹J_{CH} = 153 Hz, C3), 138.2 (d, ¹J_{CF} = 233 Hz, *p*-B(C₆F₅)₃), 137.0 (d, ¹J_{CF} = 235 Hz, *m*-B(C₆F₅)₃), 129.9 (br m, ipso-B(C₆F₅)₃), 112.2 (gated: t, ¹J_{CH} = 155 Hz, C4), 105.3, 105.2 (each C Cp), 60.9 (¹J_{CH} = 151 Hz, C2), 31.8 (¹J_{CH} = 151 Hz, C1), 10.5 (br m, *Me*-B(C₆F₅)₃) ppm. Signals of potentially coordinating THF-*d*₆ were observed at δ 68.2 and 26.1 ppm (free solvent THF-*d*₆, signals at δ 67.4 and 25.3 ppm). Data for **5'** are as follows. ¹H NMR (THF-*d*₆, 599.8 MHz, 228 K): δ 6.22 (ptd, ³J_{HH} = 11.5 Hz, 17.0 Hz, 1H, 3-H), 5.93, 5.92 (s, each 5H, Cp H), 4.58 (d, ³J_{HH} = 17.0 Hz, 1H, 4-H'), 4.46 (d, ³J_{HH} = 11.5 Hz, 1H, 4-H), 3.08 (m, 1H, 2-H), 2.95 (dd, ³J_{HH} = 10.8 Hz, ²J_{HH} = 6.2 Hz, 1H, 1-H'), 2.21 (dd, ³J_{HH} = 11.2 Hz, ²J_{HH} = 6.2 Hz, 1H, 1-H), 0.45 (br s, 3H, *Me*-B(C₆F₅)₃) ppm. 1D TOCSY NMR (THF-*d*₆, 599.8 MHz, 228 K): irradiation at δ 4.46 (4-H) ppm, response at δ 6.22 (3-H), 4.58 (4-H'), 3.08 (2-H), 2.95 (1-H'), 2.21 (1-H) ppm. ¹³C NMR (THF-*d*₆, 150.8 MHz, 228 K): δ 149.0 (d, ¹J_{CF} = 235 Hz, *o*-B(C₆F₅)₃), 148.8 (C3), 138.2 (d, ¹J_{CF} = 233 Hz, *p*-B(C₆F₅)₃), 137.0 (d, ¹J_{CF} = 235 Hz, *m*-B(C₆F₅)₃), 129.9 (br m, ipso-B(C₆F₅)₃), 110.1 (gated: t, ¹J_{CH} = 157 Hz, C4), 105.6, 105.4 (each C Cp), 50.5 (¹J_{CH} = 143 Hz, C2), 42.3 (¹J_{CH} = 157 Hz, C1), 10.5 (br m, *Me*-B(C₆F₅)₃) ppm. Data for **6** are as follows. ¹H NMR (THF-*d*₆, 599.8 MHz, 228 K): δ 6.39–6.31 (m, 2H, 2-H), 5.54 (s, 10H, Cp H), 5.24–5.17 (m, 2H, 1-H'), 5.11–5.05 (m, 2H, 1-H), 0.45 (br s, 3H, *Me*-B(C₆F₅)₃) ppm. TOCSY NMR (THF-*d*₆, 599.8 MHz, 228 K): irradiation at δ 6.35 (2-H), response at δ 5.20 (1-H'), 5.07 (1-H) ppm. ¹³C NMR (THF-*d*₆, 150.8 MHz, 228 K): δ 149.0 (d, ¹J_{CF} = 235 Hz, *o*-B(C₆F₅)₃), 138.8 (C2), 138.2 (d, ¹J_{CF} = 233 Hz, *p*-B(C₆F₅)₃), 137.0 (d, ¹J_{CF} = 235 Hz, *m*-B(C₆F₅)₃), 129.9 (br m, ipso-B(C₆F₅)₃), 118.2 (C1), 96.9 (C–Cp), 10.5 (br m, *Me*-B(C₆F₅)₃) ppm.

Photolysis of 3 in the Presence of *tert*-Butyl Isocyanide: Generation of 7a. A solution containing 30 mg (33.6 μmol) of **3** and 5.5 mg (67.3 μmol) of *tert*-butyl isocyanide in 0.8 mL of THF-*d*₆ was photolyzed (Philips HPK 125 lamp, Pyrex filter) at -78 °C for 2 h. The NMR spectra (at -45 °C) showed the formation of the product **7a** besides free butadiene and excess Me₃CN≡C. Data for **7a** are as follows. ¹H NMR (THF-*d*₆, 599.8 MHz, 223 K): δ 5.58 (s, 10H, Cp H), 1.40 (s, 9H, C(CH₃)₃), 0.49 (br s, 3H, *Me*-B(C₆F₅)₃) ppm; free *tert*-butyl isocyanide, δ 1.39 (ps, 9-H) ppm. ¹³C NMR (THF-*d*₆, 150.8 MHz, 223 K): δ 148.9 (d, ¹J_{CF} = 235 Hz, *o*-B(C₆F₅)₃), 138.2 (d, ¹J_{CF} = 233 Hz, *p*-B(C₆F₅)₃), 137.0 (d, ¹J_{CF} = 237 Hz, *m*-B(C₆F₅)₃), 129.8 (br m, ipso-B(C₆F₅)₃), 95.5 (C Cp), 57.3, 30.8 (*tert*-butyl), 10.2 (br m, *Me*-B(C₆F₅)₃) ppm.

Photolysis of 3 in the Presence of Cyclohexyl Isocyanide: Generation of 7b. A mixture of 30 mg (33.6 μmol) of **3** with 7.3 mg (67.3 μmol) of cyclohexyl isocyanide in 0.8 mL of THF-*d*₆ was photolyzed at -78 °C for 2 h analogously as described above to give **7b** and free butadiene (plus excess RNC). At room temperature **7b** was slowly converted into **8** (see below). Complex **7b** was not isolated but was characterized spectroscopically, as follows. ¹H NMR (THF-*d*₆, 599.8 MHz, 203 K): δ 5.62 (s, 10H, Cp H), 3.69–3.61 (m, 1H, [N]–CH), 2.18–2.12 (m, 2H), 1.82–1.78 (m, 2H), 1.65–1.58 (m, 1H),

1.50–1.42 (m, 2H), 1.27–1.22 (m, 2H), 1.20–1.13 (m, 1H, cyclohexyl CH₂), 0.49 (br s, 3H, *Me*-B(C₆F₅)₃) ppm. 1D TOCSY NMR (THF-*d*₆, 599.8 MHz, 203 K): irradiation at δ 3.65 ([N]–CH) ppm, response at δ 2.16, 1.80, 1.61, 1.46, 1.25, 1.15 ppm. ¹³C NMR (THF-*d*₆, 150.8 MHz, 203 K): δ 148.9 (d, ¹J_{CF} = 235 Hz, *o*-B(C₆F₅)₃), 138.2 (d, ¹J_{CF} = 233 Hz, *p*-B(C₆F₅)₃), 137.0 (d, ¹J_{CF} = 237 Hz, *m*-B(C₆F₅)₃), 129.8 (br m, ipso-B(C₆F₅)₃), 95.5 (C Cp), 63.6 ([N]–CH), 35.3, 34.5, 21.1 (cyclohexyl CH₂), 10.2 (br m, *Me*-B(C₆F₅)₃) ppm; coordinated C≡N signal not observed; free cyclohexyl isocyanide, δ 154.9 (C≡N–), 52.4 ([N]–CH), 31.4, 25.8, 19.7 (CH₂) ppm.

Synthesis of Bis(κ -Cyclohexyl isocyanide)bis(η^5 -cyclopentadienyl)tantalum Methyltris(pentafluorophenyl)borate (8). A solution containing 180 mg (202 μmol) of **3** and 88.1 mg (807 μmol) of cyclohexyl isocyanide in 0.8 mL of THF-*d*₆ was photolyzed (Philips HPK 125 lamp, Pyrex filter) at -78 °C until **3** had completely disappeared (checked by ¹H NMR). This took ca. 6 h of irradiation time. Then the sample was kept at $+60$ °C until the photolytically formed intermediate (**7b**) had completely been converted into **8** (ca. 4 h). Pentane (2 mL) was added to precipitate the product. The supernatant solvent mixture was removed and the crude product dissolved in 1 mL of dichloromethane. The product was again precipitated by the addition of 2 mL of pentane and the orange solid product **8** collected by filtration: yield of **8** 115 mg (54%); mp 123 °C. Anal. Calcd for C₄₃H₃₅N₂BF₁₅Ta (1056.5): C, 48.89; H, 3.34; N, 2.65. Found: C, 48.32; H, 3.46; N, 2.76. IR (KBr): $\tilde{\nu}$ 3131 (vw), 2938 (s), 2859 (m), 2134, 2088 (s), 1641 (m), 1510 (vs), 1456 (vs), 1363 (m), 1265 (s), 1084 (vs), 995–935 (br m), 834 (m), 806 (m) cm⁻¹. ¹H NMR (dichloromethane-*d*₂, 599.8 MHz, 298 K): δ 5.14 (s, 10, Cp H), 3.99–3.92 (m, 2H, [N]–CH), 1.94–1.86 (m, 4H), 1.70–1.60 (m, 10H), 1.47–1.40 (m, 6H, cyclohexyl CH₂), 0.49 (br s, 3H, *Me*-B(C₆F₅)₃) ppm. ¹³C NMR (dichloromethane-*d*₂, 150.8 MHz, 298 K): δ 167.5 (C≡N–), 148.3 (d, ¹J_{CF} = 235 Hz, *o*-B(C₆F₅)₃), 137.4 (d, ¹J_{CF} = 234 Hz, *p*-B(C₆F₅)₃), 136.5 (d, ¹J_{CF} = 236 Hz, *m*-B(C₆F₅)₃), 128.7 (br m, ipso-B(C₆F₅)₃), 89.4 (C Cp), 56.6 ([N]–CH), 32.9, 24.8, 22.9 (cyclohexyl CH₂), 10.1 (*Me*-B(C₆F₅)₃) ppm. ESI MS (dichloromethane-*d*₂): *m/z* 530 (100%), 447 (10%), 421 (68%), 365 (6%), 338 (14%), 311 (8%).

X-ray crystal structure analysis of **8**: single crystals were obtained by diffusion of pentane vapor into a THF-*d*₆ solution of **8**; formula C₄₃H₃₅N₂BF₁₅Ta, *M_r* = 1056.49, 0.20 × 0.20 × 0.10 mm, *a* = 11.248(1) Å, *b* = 11.481(1) Å, *c* = 17.206(1) Å, α = 108.05(1)°, β = 103.09(1)°, γ = 94.61(1)°, *V* = 2030.3(4) Å³, ρ_{calcd} = 1.728 g cm⁻³, μ = 28.11 cm⁻¹, empirical absorption correction via ψ scan data (0.934 ≤ *C* ≤ 0.999), *Z* = 2, triclinic, space group *P*1 (No. 2), λ = 0.710 73 Å, *T* = 223 K, $\omega/2\theta$ scans, 8508 reflections collected ($\pm h, \pm k, \pm l$), (sin θ)/ λ = 0.62 Å⁻¹, 8221 independent and 6390 observed reflections (*I* ≥ 2 σ (*I*)), 560 refined parameters, *R* = 0.047, *R_w*² = 0.126, maximum residual electron density 1.30 (–2.13) e Å⁻³, hydrogens calculated and refined riding. The anisotropic thermal parameters of the cyclohexyl–N≡C unit C8–N16 indicate the presence of several stereoisomers also in the crystal. Resolving the kind and ratio of these was not possible; for chemically more meaningful geometrical parameters, restraints were used, taking the other nondisordered unit as a model. All data sets were collected with Enraf-Nonius CAD4, MACH3, and KappaCCD diffractometers. Programs used: data collection, EXPRESS and COLLECT; data reduction, MoLEN and DENZO-SMN; absorption correction for CCD data, SORTAV; structure solution, SHELXS-86 and SHELXS-97; structure refinement, SHELXL-93 and SHELXL-97; graphics (with unsystematical numbering schemes), SCHAKAL-92 and DIAMOND.³⁶

Computational Details. Gradient-corrected density functional calculations were carried out, with corrections for exchange and correlation according to Becke²⁹ and Perdew,³⁰ respectively (BP86). Geometries were optimized using the

program system TURBOMOLE³¹ within the framework of the RI-*J* approximation.³² For Ta, effective core potentials (ECP-60) were applied, which include relativistic corrections.³³ A triple- ζ valence basis plus polarization (TZVP) was employed for all elements.³⁴ For the optimized geometries, a bond analysis was carried out with the ADF program package (version 2.3).³⁵ Main-group elements were described with a double- ζ -STO basis plus polarization, whereas for the transition metal a triple- ζ -STO basis was used (ADF databases III and IV, respectively). The integration accuracy parameter was

(29) (a) Becke, A. D. *J. Chem. Phys.* **1986**, *84*, 4524. (b) Becke, A. D. *J. Chem. Phys.* **1988**, *88*, 1053. (c) Becke, A. D. *Phys. Rev.* **1988**, *A38*, 3098.

(30) (a) Perdew, J. P. *Phys. Rev.* **1986**, *B33*, 8822. (b) Perdew, J. P. *Phys. Rev.* **1986**, *B34*, 7406.

(31) (a) Ahlrichs, R.; Bär, M.; Häser, M.; Horn, H.; Kölmel, C. *Chem. Phys. Lett.* **1989**, *162*, 165. (b) Treutler, O.; Ahlrichs, R. *J. Chem. Phys.* **1995**, *102*, 346. (c) Ahlrichs, R.; von Arnim, M. In *Methods and Techniques in Computational Chemistry: METECC-95*; Clementi, E., Corongiu, G., Eds.; STEF: Cagliari, Italy, 1995; p 509.

(32) (a) Eichkorn, K.; Treutler, O.; Öhm, H.; Häser, M.; Ahlrichs, R. *Chem. Phys. Lett.* **1995**, *240*, 283. (b) Eichkorn, K.; Treutler, O.; Öhm, H.; Häser, M.; Ahlrichs, R. *Chem. Phys. Lett.* **1995**, *242*, 652.

(33) Andrae, D.; Häussermann, U.; Dolg, M.; Stoll, H.; Preuss, H. *Theor. Chim. Acta* **1990**, *77*, 123.

(34) Schäfer, A.; Huber, C.; Ahlrichs, R. *J. Chem. Phys.* **1994**, *100*, 5829.

(35) (a) Baerends, E. J.; Ellis, D. E.; Ros, P. E. *Chem. Phys.* **1973**, *2*, 41. (b) teVelde, G.; Baerends, E. J. *J. Comput. Phys.* **1992**, *99*, 84. (c) Fonseca Guera, C.; Visser, O.; Snijders, J. G.; te Velde, G.; Baerends, E. J. In *Methods and Techniques in Computational Chemistry: METECC-95*; Clementi, E., Corongiu, G., Eds.; STEF: Cagliari, Italy, 1995; p 305.

set to 5.0. No symmetry constraints were employed, except when noted.

Acknowledgment. Financial support from the Fonds der Chemischen Industrie, the Bundesministerium für Bildung und Wissenschaft, Forschung und Technologie, the Deutsche Forschungsgemeinschaft, and the Swiss National Science Foundation is gratefully acknowledged.

Supporting Information Available: Figures and tables giving details of the X-ray crystal structure analyses of the complexes **4b,c** and **8**, figures and tables giving additional NMR information, and a listing of Cartesian coordinates of optimized geometries, together with the corresponding total energies, for complexes **I–V**. This material is available free of charge via the Internet at <http://pubs.acs.org>.

OM990215L

(36) (a) EXPRESS: Nonius BV, 1994. (b) COLLECT: Nonius BV, 1998. (c) MolEN: Fair, K. Enraf-Nonius BV, 1990. (d) DENZO-SMN: Otwinowski, Z.; Minor, W. *Methods Enzymol.* **1997**, *276*, 307. (e) SORTAV: Blessing, R. H. *Acta Crystallogr.* **1995**, *A51*, 33. Blessing, R. H. *J. Appl. Crystallogr.* **1997**, *30*, 421. (f) SHELXS: Sheldrick, G. M. *Acta Crystallogr.* **1990**, *A46*, 467. (g) SHELXL: Sheldrick, G. M. Universität Göttingen, 1997. (h) SCHAKAL: Keller, E. Universität Freiburg, 1997. (i) Brandenburg, K. Universität Bonn, 1996.